A novel nematode species from the Siberian permafrost shares adaptive mechanisms for cryptobiotic survival with *C. elegans* dauer larva

Anastasia Shatilovich[1#], Vamshidhar R. Gade[2,9#], Martin Pippel[3], Tarja T. Hoffmeyer[4], Alexei V. Tchesunov[5], Lewis Stevens[6], Sylke Winkler[2,7], Graham M. Hughes[8], Sofia Traikov[2], Michael Hiller[3,10], Elizaveta Rivkina[1], Philipp H. Schiffer[4*], Eugene W Myers[3], Teymuras V. Kurzchalia[2*]

1. Institute of Physicochemical and Biological Problems in Soil Science RAS, Pushchino, Russia
2. Max Planck Institute for Molecular Cell Biology and Genetics, Dresden, Germany
3. Center for Systems Biology, Dresden, Germany
4. Institute for Zoology, University of Cologne
5. Department of Invertebrate Zoology, Faculty of Biology, M.V. Lomonosov Moscow State University, Moscow, Russia
6. Tree of Life, Wellcome Sanger Institute, Cambridge, UK
7. DRESDEN concept Genome Center, Dresden, Germany
8. School of Biology and Environmental Science, University College Dublin, Belfield, Dublin, Ireland
9. Institute of Biochemistry, ETH Zürich, 8093 Zürich, Switzerland
10. LOEWE Centre for Translational Biodiversity Genomics, Senckenberg Society for Nature Research & Goethe University, Frankfurt am Main, Germany

[#] A.S and V.G contributed equally to this work

*To whom correspondence may be addressed

Email: kurzchalia@mpi-cbg.de

p.schiffer@uni-koeln.de

Abstract

Some organisms in nature have developed the ability to enter a state of suspended metabolism called cryptobiosis[1] when environmental conditions are unfavorable. This state-transition requires the execution of complex genetic and biochemical programs[1,2,3], that enables the organism to survive for prolonged periods. Recently, nematode individuals have been reanimated from Siberian permafrost after remaining in cryptobiosis. Preliminary analysis indicates that these nematodes belong to the genera *Panagrolaimus* and *Plectus*[4]. Here, we present precise radiocarbon dating indicating that the *Panagrolaimus* individuals have remained in cryptobiosis since the late Pleistocene (~46,000 years). Phylogenetic inference based on our genome assembly and a detailed morphological analysis demonstrate that they belong to an undescribed species, which we named *Panagrolaimus n. sp*. Comparative genome analysis revealed that the molecular toolkit for cryptobiosis in *Panagrolaimus n. sp.* and in *C. elegans* is partly orthologous. We show that biochemical mechanisms employed by these two species to survive desiccation and freezing under laboratory conditions are similar. Our experimental evidence also reveals that *C. elegans* dauer larvae can remain viable for longer periods in suspended animation than previously reported. Altogether, our findings demonstrate that nematodes evolved mechanisms potentially allowing them to suspend life over geological time scales.

Introduction

Organisms from diverse taxonomic groups can survive extreme environmental conditions, such as the complete absence of water or oxygen, high temperature, freezing, or extreme salinity. The survival strategies of such organisms include a state known as suspended animation or cryptobiosis, in which they reduce metabolism to an undetectable level[6]. Spectacular examples of long-term cryptobiosis include a *Bacillus* spore that was preserved in the abdomen of bees buried in amber for 25 to 40 million years[7], and a 1000 to 1500 years-old *Lotus* seed, found in an ancient lake, that was subsequently able to germinate[8]. Metazoans such as tardigrades, rotifers and nematodes are also known for remaining in cryptobiosis for prolonged periods[9,10]. The longest records of cryptobiosis in nematodes are reported for the Antarctic species *Plectus murrayi*[11] (25.5 years in moss frozen at -20°C), and *Tylenchus polyhypnus*[12] (39 years desiccated in a herbarium specimen).

Intensive research during the last decades has demonstrated that permafrosts (perennially frozen sediments) are unique ecosystems preserving life forms at sub-zero temperatures over thousands of years[13,14,15,16]. Permafrost remains are an exceptional source for discovering a wide variety of unicellular and multicellular living organisms surviving in cryptobiosis for prolonged periods[6,17,18]. We recently reanimated soil nematodes that were preserved in Siberian permafrost for potentially thousands of years, and initial morphological observations provisionally described them as belonging to the genera *Panagrolaimus* and *Plectus.* Previous studies demonstrated several species of *Panagrolaimus* can undergo cryptobiosis in the form of anhydrobiosis (through desiccation) and cryobiosis (through freezing)[19,20,21,22,23]. In various nematodes, entry into anhydrobiosis is often accompanied by a preparatory phase of exposure to mild desiccation, known as preconditioning[21,24]. This induces a specific remodelling of the transcriptome, the proteome, and metabolic pathways that enhances survival ability[2,3,25]. Some panagrolaimids evolved adaptive mechanisms for rapid desiccation where most of the cellular water is lost, while others evolved freezing tolerance, without loss of water, at sub-zero temperatures by inhibiting the growth and recrystallisation of ice crystals[21]. However, the genetic and biochemical mechanisms of long term cryptobiosis in these organisms have not yet been investigated in detail.

Here we present a high-quality genome assembly and a detailed morphological, phylogenetic analysis and define a novel species, *Panagrolaimus n. sp.* Precise radiocarbon dating indicates that *Panagrolaimus n. sp* remained in cryptobiosis for about 46,000 years, since late Pleistocene. Furthermore, making use of the powerful model organism *C. elegans*,

we demonstrate that *Panagrolaimus* and *C. elegans* dauer larvae utilize similar adaptive mechanisms to survive extreme desiccation and freezing, i.e. upregulation of trehalose biosynthesis and gluconeogenesis.

Results

Discovery site and radiocarbon dating

Previously, we showed that nematodes from the Siberian permafrost with morphologies consistent with the genera *Panagrolaimus* and *Plectus* could be reanimated thousands of years after they had been frozen in the permafrost. Several viable nematode individuals were found in two out of more than 300 studied samples of permafrost deposits of different ages and genesis, collected by researchers of the Soil Cryology Lab, Pushchino, Russia, in the course of perennial paleo-ecological expeditions carried out in the coastal sector of the northeastern Arctic[17]. The detailed description of the study site (outcrop Duvanny Yar, Kolyma River, Fig.1A), sampling and revitalizing procedures are provided in Supplementary Information (SI). Like other late Pleistocene permafrost formations in the northeastern Arctic, Duvanny Yar comprises permanently frozen ice-rich silt deposits riddled with large polygonal ice wedges and divided by them into mineral blocks[26,27] (Fig.1B). The sediments include sandy alluvial layers, peat lenses, buried paleosols and Pleistocene rodent burrows (Fig.1C). The burrow (P-1320), in which *Panagrolaimus* nematodes were found (Fig.1D), has been taken from the frozen outcrop wall at a depth of about 40 m below the surface and about 11 m above river water level in undisturbed and never thawed late Pleistocene permafrost deposits. The fossil burrow left by arctic gophers of the genus *Citellus* consists of entrance tunnel and a large nesting chamber up to 25 cm in diameter[26].

The sterility of permafrost sampling and age of cultivated biota were discussed in detail in several reviews[14,28, 29]. Based on previous reports, the age of the organisms found in a burrow is equal to the freezing time and corresponds to the age of organic matter conserved in the syncryogenic sediments. This makes it possible to use radiocarbon dating of organic matter to establish the age of organisms. We performed Accelerator Mass Spectrometry (AMS) radiocarbon analysis of plant material obtained from studied borrow P-1320 and determined a direct ^{14}C age of 44,315±405 BP (Institute of Geography, RAS; sample $IGAN_{AMS}$ 9137). Calibrated age range is 45,839 – 47,769 cal BP (95.4% probability) (Fig.S1).

Like other parthenogenetic *Panagrolaimus* the newly discovered species is triploid

The revived animal was cultivated in the laboratory for over 100 generations and initially described as *Panagrolaimus* aff. d*etritophagus*[4] based on morphology. We conducted a detailed morphological analysis of the revived animal (Fig.2, S2, Table S1;BOX1), which confirmed unambiguously that the animal belongs to the genus of *Panagrolaimus*, in agreement with a previous phylogenetic analysis of the 18S ribosomal RNA sequence[4]. However, due to the morphological uniformity of *Panagrolaimus*, unusual even for nematodes, morphology and molecular analysis of a single ribosomal RNA sequence is insufficient to describe a species. We found the species to be parthenogenetic, which further complicates description under most species concepts.

To obtain comprehensive molecular data for species determination using phylogenomics, we generated a genome assembly. Using PacBio HiFi sequencing, we generated 84X coverage in long reads (average length 14,425 bp). Our analysis of repeat and gene content is described in Supplementary Table 3. K-mer analysis of the reads clearly indicated that this animal has a triploid genome (Fig.3A), similar to other parthenogenetic *Panagrolaimus* species[30]. Despite the challenges that a triploid genome poses for assembly, we obtained a highly-contiguous contig assembly of the three pseudohaplotypes that comprise about 266 Mb and thus have a similar genome size as other parthenogenetic *Panagrolaimus* species[30]. The contig N50 value of all three pseudohaplotypes is 3.8 Mb. Since the three pseudohaplotypes exhibited a noticeable degree of divergence, we further investigated their relationship by using the apparent homeologs in our gene predictions to align long continuous contigs based on micro synteny (Fig. 3B). Links between the contigs clearly shows the triploid state of the genome.

166 **BOX 1 Description of *Panagrolaimus n. sp* sp. nov.**

Description	Body spindle-shaped and usually almost straight after fixation (Fig.2a, b). Cuticle thin and faintly annulated, 10–11 annules per 10 µm in cervical region, 13–14 in midbody, preanally again 10 annules withi 10 µm. Conspicuous convex lateral fields with three incisures 1.5-2 µm wide extended along the body from about ¼–1/3 procorpus length to 2/3 of tail length. In SEM, the lateral field looks as a bolster with a narrow median split. Labial region set off. Mouth opening surrounded with six lips (Fig.2c, d). Anterior sensilla as papillae arranged in two close but separate subsequent circles. Somatic sensilla (i.e., deirids and phasmids) not evident.Buccal cavity cylindro-conoid, and unarmed; its total length 9–13 µm, maximum stoma width 1.7–2.8 µm (Fig.2e). Dorsal stoma wall (dorsal rhabdion) more clearly sclerotized. Anterior part of the buccal cavity comprising cheilostom and gymnostom nearly cylindroids while stegostom conically narrowed and ended with a distinct tight flexion. Pharynx consists of three distinct parts: straight anterior procorpus, narrow medial isthmus and rounded terminal bulb. Procorpus gradually widening to it posterior end, always straight in all specimens, with transversal muscular striation, more prominent in posterior three fourths. Isthmus narrow, cylindroid, bent starkly in nearly all studied specimens. Terminal bulb strongly muscular, with a valvular apparatus at about 40% of the bulb length. Cardia in shape of truncate cone. Intestine (midgut) tissue filled with vacuoles and granules; in the anteriormost region, the granules smaller and look more pallid. Cell borders not visible in the intestine, but internal lumen distinct, sinusoid. No internal content visible in the internal lumen. Ventral excretory-secretory pore and its cuticularized duct situated at the level of anterior part of the bulb. No other details of the excretory-secretory system visible. Vulval lips protruding. Genital branch monodelphic prodelphic and situated dorsally and to the right of the midgut (Fig.2f). Vagina distinctly cuticularized and opens to the elongate uterus. A long oviduct extended anteriad from the anterior uterus; the oviduct folded up and then posteriorward and transforms into an elongate ovary. There are

	one or two ripe eggs in the uterus in most specimens. Tail short conical, with short acute spike-like mucro (Fig.2g).
Etymology	Species name *kolymaensis* (Latin) is derived from the Kolyma River area.
Holotype	Senckenberg Natural History Museum, Frankfurt am Main, Germany (collection number SMF 17067).
Paratypes	Senckenberg Natural History Museum, Frankfurt am Main, Germany (collection numbers SMF 17068, SMF 17069) (eighteen paratypes).
Type locality	Frozen fossil rodent burrow buried in permafrost 45,839 – 47,769 cal BP , 40 meters from the surface, outcrop Duvanny yar, Kolyma River, North-East of Siberia, Russia (68° 37′ 739″ N, 159° 11′ 678″ E). Frozen material from burrow was collected by Dr.S.Gubin (Soil Cryology Lab, Pushchino, Russia) in august 2002.

Phylogenomics to define *Panagrolaimus n. sp* sp. nov.

To place the species in the genus *Panagrolaimus*, we conducted a broader multi-gene phylogenomic analysis using Maximum likelihood methods. Our analysis of a concatenated, partitioned alignment of 60 genes, and a coalescence-based approach using a broader set of 12,295 gene trees, retrieves the novel species as sister to all other sequenced *Panagrolaimus* species, but as an ingroup to *Propanagrolaimus*[31] (Fig.3C; Fig. S3B-C). Thus, the phylogenetic placement provides strong evidence that this animal belongs to a novel species. Further supporting this, there is substantial sequence divergence between this novel species, and *Panagrolaimus* sp. PS1159 and *Panagrolaimus* sp. ES5, estimated to be on average 2.06 and 2.11 amino acid substitutions per site in our concatenated alignment, respectively. The substantial divergence is in line with previous data on ages of *Panagrolaimus* nematodes[30], and more broadly seen in nematodes, which can be hyper-diverse[32,33]. Our data also contradicts the assumption that parthenogenesis is monophyletic trait[30] in the *Panagrolaimus* genus (Fig.3C). Based on the Kolyma River location where the animal was unearthed, we propose the following taxonomic classification and species name:

Phylum Nematoda Potts, 1932

Class Chromadorea Inglis 1983

185 Suborder Tylenchina Thorne, 1949
186 Family Panagrolaimidae Thorne, 1937
187 *Panagrolaimus n. sp* sp. nov.

188 **_C. elegans_ dauer larvae and _Panagrolaimus n. sp._ utilize similar mechanisms to enter and**
189 **remain in cryptobiotic state for prolonged periods of time**

190 In the absence of established genetic methods in *Panagrolaimus n. sp.* we referred to *C. elegans*
191 as a powerful model system to gain insights into possible pathways for long term survival[3,4,24,25].
192 The high-quality genome of *Panagrolaimus n. sp.* allowed us to compare its molecular toolkit
193 for cryptobiosis with that of *C. elegans*. We used orthology clustering and phylogenetics to
194 investigate whether the genome of *Panagrolaimus n. sp.* contains genes previously implicated
195 in cryptobiosis in the *C. elegans* dauer larva. Our analysis showed that the *Panagrolaimus n.*
196 *sp.* genome encodes orthologs to a *C. elegans* trehalose phosphate synthase gene (*tps-2*) and to
197 a trehalose phosphatase gene (*gob-1*) (Fig. 3D, supplementary file Orthology analysis).
198 Furthermore, we found orthologs to all *C. elegans* enzymes required for polyamine
199 biosynthesis, the TCA cycle, glycolysis, gluconeogenesis, and glyoxylate shunt (Fig.3D,
200 supplementary file Orthology analysis) suggesting that *Panagrolaimus n. sp.* utilizes a similar
201 molecular tool kit as *C. elegans* to facilitate survival of unfavorable conditions.

202 Our earlier findings established that among several developmental stages of *C. elegans*,
203 only the dauer larva, formed during unfavorable conditions (such as low nutrients and high
204 population density) could survive anhydrobiosis and freezing[4,24]. To survive extreme
205 desiccation, *C. elegans* dauer larvae need to be first preconditioned at high relative humidity
206 (98% RH) for 4 days[24]. During preconditioning, dauer larvae upregulate trehalose biosynthesis
207 that ensures their survival to harsh desiccation[24,25]. We tested whether preconditioning also
208 facilitates survival of *P. kolymaensis*. Although a small proportion of *Panagrolaimus n. sp.*
209 individuals survive harsh desiccation and freezing without preconditioning (Fig.4A), mixed
210 populations of *Panagrolaimus n. sp.* survive significantly (p value< 0.0001) higher to harsh
211 desiccation upon preconditioning (Fig.4A). Similarly, preconditioning and desiccation further
212 enhanced survival rate of *Panagrolaimus n. sp.* to freezing (-80°C). Like *C. elegans,*
213 *Panagrolaimus n. sp.* upregulate trehalose levels up to 20-fold upon preconditioning (Fig.4B).
214 We previously reported that, to upregulate trehalose levels upon preconditioning, *C. elegans*
215 dauer larva dissipate their fat reserves (Triacylglycerols) by activating the glyoxylate shunt and
216 gluconeogenic pathway[25]. Upon preconditioning, we found that triacylglyceride (TAG) levels
217 are significantly decreased in *Panagrolaimus n. sp.* (Fig.S5A&B). To further investigate
218 whether the acetyl-CoA derived from degradation of TAGs culminate in trehalose, we applied

219 the previously developed method of metabolic labelling with ^{14}C-acetate in combination with
220 2D-TLC [4,25]. As shown in Fig. 4C, preconditioning led to huge increase of radioactivity in
221 trehalose and to smaller extent in some amino acids (glycine/serine, phenylalanine; panels c
222 and d). Interestingly, *Panagrolaimus n. sp.* displayed an additional spot (Fig. 4D, enumerated
223 as 7), that was not found in *C. elegans*, which we identified as trehalose-6-phosphate (Fig.S5C-
224 H), an immediate precursor of trehalose, using mass spectrometry. Thus, to resist harsh
225 desiccation, like *C. elegans*, *Panagrolaimus n. sp.* utilizes glyoxylate shunt and consequently
226 acetate derived from TAGs to synthesize trehalose. Detection of the immediate precursor
227 (trehalose-6-phosphate) suggests the flux of metabolites is intense in the latter.

228 Finally, we investigated whether *C. elegans* can also survive in prolonged cryptobiotic
229 state. Despite of preconditioning, the survival ability of desiccated dauer larvae at room
230 temperature declines very rapidly, with most larvae dead after around 10 days (Fig. 4E) (Fig.
231 S4A&B). Direct freezing at -80℃, leads to almost instant death of the animals. To test whether
232 combining these conditions could extend the viability of dauer larvae (Fig. S4A&B), we
233 transferred the desiccated larvae to -80℃. Remarkably, under these conditions, there was no
234 significant decline in viability even after 480 days (Fig. 4E). Moreover, after thawing, the
235 animals resumed reproductive growth and produced progeny in numbers like those of animals
236 kept under control conditions (Fig. 4F). Since no reduction in survival was observed at any
237 time point in extended experiments, these results suggest that the combination of anhydrobiosis
238 and freezing can prolong the survival ability of dauer larvae. Thus, *C. elegans*, when exposed
239 to combination of cryptobiotic states can survive for extremely long periods of time.

240 **Discussion**

241 Our findings here demonstrate the ability of the nematodes to survive in suspended animation
242 for geological time scales. Along with the adaptive mechanisms of an organism, a naturally
243 preserving ecosystem would synergistically aid the survival for prolonged periods. The
244 Siberian permafrost is a unique repository for preserving organisms in sub-zero temperatures
245 for millions of years. Expeditions in the past decade revived several organisms across various
246 taxa from the Siberian permafrost[5,34,35,36]. The possibility to exploit permafrost as a source for
247 reanimating multicellular animals was recognized already in 1936. A viable Cladocera
248 crustacean *Chydorus sphaericus* preserved in the Transbaikalian permafrost for several
249 thousand years[37,38] was discovered by P.N. Kapterev, who worked at the scientific station
250 Skovorodino as a GULAG prisoner. Unfortunately, this extraordinary observation remained
251 unnoticed for many decades.

The new species can now be placed into the genus *Panagrolaimus*[39], which contains several described and undescribed parthenogenetic and gonochoristic species and strains[30,40]. Many *Panagrolaimus* display adaptation to survival in harsh environments[21] and the genus includes the Antarctic species *P. davidii*[22]. The genus *Panagrolaimus* is exceptional in its morphological uniformity even among nematode species that are hard to classify based on morphology in general. Thus, species designation via microscopic (including SEM) analysis is unreliable, which is further complicated by the absence of males in parthenogenetic species makes. Males have important diagnostic features as spicules and pericloacal papillae, females differ from one species to another mainly by morphometrics, whereby the interspecies differences (absolute measures and ratios) may be very fine. Our specimens are close by absolute sizes and ratios to females of the bisexual species *Panagrolaimus detritophagus*[41]. The only non- overlapping morphometric character is index "b" (body length: pharynx length): 5.6–6.8 in *Panagrolaimus n. sp.* versus 4.4-5.1 in *P. detritophagus*.

Consequently, we turned to phylogenomics methods to place the species on the tree. This showed that species is an outgroup to other known *Panagrolaimus* species, raising for the possibility of a second independent evolution of parthenogenesis in the genus, in contrast to previous findings[40,31,30]. This will need to be confirmed through further sampling and genome sequencing of *Panagrolaimus* species. We found *Panagrolaimus n. sp.* to be triploid and thus a hybrid origin is possible, as seen in other parthenogenetic *Pangrolaimus*[30]. The highly contiguous genome of *Panagrolaimus n. sp.* will allow for analyses of this trait in comparison to other *Panagrolaimus* species currently being genome sequenced. The successful phylogenomic species identification we conducted here demonstrates the utility of this method for morphologically hard to identify species, in particular when the additional data yielded by a fully sequenced genome are considered.

Our results provide a deeper insight into the homology of molecular and biochemical mechanisms between *C. elegans* and *P. kolymaensis*, which are not only taxonomically but also ecologically distinct. *C. elegans* can mostly be found in rotting fruits and plants in temperate regions[42,43], while *Panagrolaimus* species are globally distributed and prevalent in leaf litter and soil[40], including in harsh environments[21]. We show through orthology analysis that the well-studied molecular pathways used by *C. elegans* larvae to enter the dauer state, such as insulin[44,45] (DAF-11, DAF-2 & DAF-16), TGF-β[46] (DAF-7), steroid[47] (DAF-9, DAF-12) are present in the genome of the *Panagrolaimus n. sp.* (Fig.S4C). While further functional

analyses are needed to study molecular pathways detail, our results hint at convergence or parallelism in the molecular mechanisms organizing dauer formation and cryptobiosis.

As mentioned earlier preconditioning enhances the survival of *Panagrolaimus n. sp.* to desiccation and freezing. We previously reported that preconditioning induces trehalose upregulation in *C. elegans* dauer larvae and the elevated trehalose renders desiccation tolerance by protecting the cellular membranes[24]. It is not surprising that *Panagrolaimus n. sp.* upregulates trehalose, however the magnitude of trehalose elevation is higher than *C. elegans* dauer larvae. This indicates that central regulators (DAF-16, DAF-12) of trehalose upregulation may differentially regulate *tps-2* in *Panagrolaimus n. sp* [48,49]. Although *Panagrolaimus n. sp.* utilizes glyoxylate shunt and gluconeogenesis to upregulate trehalose levels, it is intriguing to observe that they accumulate substantial levels of trehalose-6-phosphate. Further investigation of this observation using perturbation experiments will provide insights into metabolic regulation in *Panagrolaimus n. sp.* upon preconditioning. Our findings for the first time demonstrate that *C. elegans* dauer larvae possess an inherent ability to survive freezing for prolonged periods if they undergo anhydrobiosis. It is tempting to speculate that undergoing anhydrobiosis might be a survival strategy of *C. elegans* to survives seasonal changes in nature.

In summary our findings indicate that by adapting to survive cryptobiotic state for short time frames in environments like permafrost, some nematode species gained the potential for individual worms to remain in the state for geological timeframes. This raises the question whether there is an upper limit to the length of time an individual can remain in the cryptobiotic state, potentially only limited by drastic changes to the environment such as strong fluctuations in ambient temperature, natural radioactivity, or other abiotic factors. These findings have implications for our understanding of evolutionary processes, since generation times could be stretched from days to millennia, species ages might be much longer than anticipated, and long-term survival of individuals of species can lead to the refoundation of otherwise extinct lineages. Finally, understanding the precise mechanisms of long-term cryptobiosis and cues that lead to successful revivals can inform new methods for long term storage of cells and tissues.

313 **Methods**

314 **Materials and *C. elegans* strains**

315 [1-14C] -acetate (sodium salt) from Hartmann Analytic (Braunschweig, Germany). All other
316 chemicals were purchased from Sigma-Aldrich (Taufkirchen, Germany). The *Caenorhabditis*
317 Genetic Centre (CGC) provided *daf-2(e1370)* and *E. coli NA22* strains.

318

319 **Genomic DNA isolation from *Panagrolaimus n. sp* nematodes**

320 *Panagrolaimus n. sp.* nematodes were grown on several plates of NGM agar plated with *E.*
321 *Coli NA22* bacteria at 20°C. Worms were collected from the plates, washed with water at least
322 three to five times by centrifugation at 1000 g to remove any residual bacteria and any debris.
323 The worm pellet was dissolved in 5 volumes of worm lysis buffer (0.1M Tris-HCl pH=8.5,
324 0.1M NaCl, 50mM EDTA pH=8.0) and distributed in 1.5 ml of microcentrifuge tubes. These
325 tubes are incubated at -80°C for 20 minutes. 100 µl of Proteinase 'K' (20 mg/ml) was added to
326 each tube and they are incubated at 60°C overnight. 625 µl of cold GTC buffer (4M
327 Guanidinium Thiocynate, 25mM Sodium citrate, 0.5% (v\v) N-lauroylsarcosine, 7%(v/v) Beta
328 Mercaptoethanol) was added to the tube, incubated on ice 30 min, and mixed by inverting every
329 10 min. 1 volume of phenol–chloroform-isoamyl alcohol (pH=8) was added to the lysate and
330 mixed by inverting the tube 10-15 times. Tubes were centrifuged for 5 min at 10,000 g at 4 °C
331 to separate the phases. The upper aqueous phase was carefully collected into a fresh tube. One
332 volume of fresh chloroform was added and mixed by inverting the tubes for 10-15 times and
333 centrifuged for 5 min at 10,000 g at 4°C to separate the phases. One volume of cold 5 M NaCl
334 was added, mixed by inverting the tubes and incubated on ice for 15 min. After incubation
335 these tubes were centrifuged for 15 min at 12,000–16,000 g at 4 °C. The supernatant containing
336 the nucleic acids were slowly transferred into a fresh tube. One volume of isopropanol was
337 added to the tube, inverted few times, and incubated on ice for 30 minutes. After incubation,
338 the tubes were centrifuged at 3000 g for 30–45 min at 25°C and the supernatant was discarded
339 without disturbing the pellet. The pellet was washed twice with 1 ml of 70% ethanol, tubes
340 were centrifuged at 3000 g for 5 min and supernatant was discarded and incubated at 37°C for
341 10-15 min to dry the pellet. The pellet was resuspended carefully in TE buffer. The quality of
342 the genomic DNA was analyzed with pulse field gel electrophoresis.

343

344

345

346 **Genome sequencing and assembly**

347 Long insert library has been prepared as recommended by Pacific Bioscienes according to
348 theprotocol 'Procedure & Checklist-Preparing gDNA Libraries Using the SMRTbell® Express
349 Template Preparation Kit 2.0'. In summary, RNAse treated HMW gDNA has been sheared to
350 20Kb fragments on the MegaRuptor™ device (Diagenode) and 10 µg sheared gDNA have
351 been used for library preparation. The PacBio SMRTbell™ library was size selected in two
352 fractions (9-13kb, > 13kb) using the BluePippin™ device with cassette definition of 0.75% DF
353 MarkerS1 3-10 kb Improved Recovery. The second fraction of the size selected library has
354 been loaded with 95 pM on plate on a Sequel SMRT cell (8M). Sequel polymerase 2.0 has
355 been used in combination with the v2 PacBio sequencing primer and the Sequel sequencing kit
356 2.0EA, runtime was 30 hours. We created PacBio CCS reads from the subreads.bam file using
357 PacBio's ccs command linetool (version4.2.0). We obtained 8.5Gb hiqh quality CCS reads
358 (HiFi reads) with a N50 of 14.4 Kb. We ran HiCanu (version 2.2)[39] to create the contig
359 assembly. Blobtools (version 1.1.1,CITE:) was used to identify and remove bacterial contigs.
360 The final triploid contig assembly consists of 856 contigs has a N50 of 3.82 Mb and a size of
361 266Mb. The mitochondrial genome was created with the mitoHifi pipeline (version
362 2, https://github.com/marcelauliano/MitoHiFi) based on the assembled contigs and the closely
363 related reference mitochondrial genome of Panagrellus redivivus (strain: PS2298/MT8872,
364 ENAaccession: AP017464). The mitoHifi pipeline identified 49 mitochondrial contigs ranging
365 from 13-32Kb. The final annotated circular mitochondrial genome has length of 17467 bp.
366 To identify pseudohaplotypes in the *P. kolymanensis* sp. nov genome assembly, we selected
367 the longest isoform of each predicted protein-coding gene in our assembly and in the *C. elegans*
368 genome (downloaded from WormBase Parasite, release WBPS15) using AGAT (version 0.4.0)
369 and clustered them into orthologous groups (OGs) using OrthoFinder (version 2.5.2). We
370 identified OGs that contained three *Panagrolaimus* sequences (i.e. groups that were present as
371 single-copy in all three pseudohaplotypes) and used these to identify trios of multi-megabase
372 size contigs derived from the three pseudohaplotypes. We visualized synteny between the three
373 pseudohaplotypes using Circos to plot the positions of each homeolog (version 0.69-8).
374

375 **Genome annotation**

376 We used RepeatModeler 1.0.8 (http://www.repeatmasker.org/) with parameter '-engine ncbi'
377 to create a library of repeat families. This library was used with RepeatMasker 4.0.9 to soft-
378 mask the *Panagrolaimus* genome. To annotate genes, we cross mapped protein models from

379 an existing *Panagrolaimus* as external evidence in the Augustus[51] based pipeline. We evaluated
380 the completeness of our predictions using BUSCO on the gVolante web interface.
381
382 **Orthology analysis**
383 We conducted a gene orthology analysis using genomic data from *Panagrolaimus n. sp*, the
384 plectid nematode species from the permafrost, as well as genomic data from WormBase
385 Parasite (https://parasite.wormbase.org; accessed 17/12/2020): *Caenorhabditis elegans*,
386 *Diploscapter coronatus*, *Diploscapter pachys*, *Halicephalobus mephisto*, *Panagrellus*
387 *redivivus*, *Panagrolaimus davidi*, *Panagrolaimus* sp. ES5, *Panagrolaimus* sp. PS1159,
388 *Panagrolaimus superbus*, *Plectus sambesii*, and *Propanagrolaimus* sp. JU765. For plectids,
389 genomic resources are scarce. We therefore added transcriptome data of *Plectus murrayi*,
390 *Anaplectus granulosus*, *Neocamacolaimus parasiticus*, and *Stephanolaimus elegans*. The latter
391 three transcriptomes were kindly provided by Dr. Oleksandr Holovachov (Swedish museum of
392 natural history). The *Anaplectus granulosus*, and *Neocamacolaimus parasiticus* transcriptomes
393 have been published [52,53]. All three transcriptomes were assembled de novo with Trinity[54]. The
394 exact procedures are described in the respective publications[52,53] . The *Stephanolaimus* elegans
395 transcriptome was assembled in the same way as described for *Neocamacolaimus parasiticus*.
396 The *Plectus murrayi* transcriptome was built from raw reads deposited at NCBI (https://sra-
397 downloadb.be-md.ncbi.nlm.nih.gov/sos2/sra-pub-run-13/SRR6827978/SRR6827978.1;
398 accessed 22.12.2020). The transcriptome was assembled using Galaxy Trinity version 2.9.1[55],
399 [54] using all default options and including in silico normalization of reads before assembly.
400 Transdecoder (conda version 5.5.0)[56] was used to translate to amino acid sequence. Identical
401 reads were removed with cd-hit version 4.8.1[57,58], and the Trinity
402 get_longest_isoform_seq_per_trinity_gene.pl command[56] (Trinity conda version 2.8.5)
403 {Anaconda Software Distribution, Conda, Version 4.9.2, Anaconda, Nov. 2020; was used, to
404 remove shorter isoforms. Amino acid translated longest isoforms from genomic data were
405 extracted with AGAT {Dainat, https://www.doi.org/10.5281/zenodo.3552717} from genome
406 assembly FASTA files and genome annotation GFF3 files, using the
407 agat_convert_sp_gxf2gxf.pl command to convert all GFF3 files to the required GFF3 format,
408 and the agat_sp_keep_longest_isoform.pl as well as the agat_sp_extract_sequences.pl
409 commands to extract amino acid translated FASTA files. The headers and names of all FASTA
410 files were modified to allow for simple species assignment of each sequence in subsequent
411 analysis. The orthology analysis was conducted with OrthoFinder v. 2.5.1[59,60] using default
412 settings. For genes of interest, we constructed alignments with MAFFT v. 7.475[61] using the

413 localpair and maxiterate (1000) functions. We removed spurious sequences and areas that were
414 not well aligned with Trimal v. 1.4.rev22[62] (procedure stated in supplementary file Orthology
415 analysis below each phylogeny). We then ran phylogenetic analysis with Iqtree2 v. 2.0.6[63],
416 with -bb 1000 option, testing the model for each analysis (models eventually used stated in
417 supplementary file Orthology analysis). We also checked for PFAM domains using
418 Interproscan v. 5.50-84.0[64]. Part of the analysis was performed on the HPC RRZK CHEOPS
419 of the Regional Computing Centre (RRZK) of the University of Cologne. The phylogenies
420 were visualized with Dendroscope 3.7.6[65] and figures were created with Inkscape
421 {https://inkscape.org}.
422
423 **Phylogenomics**
424 Sequences of 18S and 28S genes from 44 taxa across the *Propanagrolaimus*, *Panagrolaimus*,
425 *Panagrellus* and *Halicephalobus* genera were aligned (MAFFT L-INS-I v7.475)[61],
426 concatenated [66]and used to infer a species tree using maximum likelihood via (IQTREE)[67] and
427 partitioned by best-fit models of sequence evolution for both[68]. Nodal support was determined
428 using 1000 bootstrap pseudoreplicates. A further 60 genes from 101 taxa were used to confirm
429 the taxonomic position using the supermatrix concatenation methods outlined above. Given the
430 limitations of differential gene sampling, we expanded our phylogenomic analyses to include
431 a coalescence approach using 12,295 ML gene trees inferred for orthogroups containing the
432 target animal. Instances of multiple genes per species per group were treated as
433 paralogs/orthologs and analysed using ASTRAL-Pro[69].
434
435 **Desiccation survival assay**
436 *C. elegans* dauer larvae desiccation assays were performed as described in. *Panagrolaimus n.*
437 *sp* desiccation assays were performed with mixed populations of the worms.
438
439 **Exposure of nematodes to extreme environments**
440 Dauer larvae or *Panagrolaimus n. sp* nematodes were preconditioned and desiccated as
441 described[24] and then transferred to elevated temperature of 34°C, freezing (-80°C) and anoxia.
442 Anoxic environment was generated in a desiccation chamber at 60%RH by flushing the
443 Nitrogen gas into the chamber. The concentration of oxygen inside the chamber was monitored.
444 After each timepoint they were rehydrated with 500 µl of water for 2-3 hours. Rehydrated
445 worms were transferred to NGM agar plates with *E. Coli NA22* as food. Survivors were counted

446 after overnight recovery. Each experiment was performed on two different days with at least
447 two technical replicates.
448
449 **Trehalose quantification from nematode lysates**
450 Trehalose measurements were performed as described in previous reports[25].
451
452 **Radiolabeling, metabolite extraction and 2D-TLC**
453 The above-mentioned procedures were performed according to previous reports[3,25].

454 **Identification of trehalose-6-phosphate from TLC plates**
455 Normalised aqueous fractions from the non-preconditioned and preconditioned samples were
456 separated by high performance thin layer chromatography (HPTLC), using 1-propanol-
457 methanol-ammonia (32%)-water (28:8:7:7 v/v/v/v) as first, dried for 15 min and 1-butanol-
458 acetone-glacial acetic acid–water (35:35:7:23 v/v/v/v) second dimension respectively. Using
459 the trehalose as a standard on both dimensions of the TLC, the regions of interest were scrapped
460 out from the TLCs. The scraped-out silica was extracted with 10 ml of 50% methanol twice.
461 The fractions were combined, dried under vacuum and dissolved in 100 µl of Ms mix solution
462 containing 4:2:1 (Isopropanol:Methanol:Chloroform) with 7.5 mM ammonium formate. Mass
463 spectrometric analysis was performed on a Q Exactive instrument (Thermo Fischer Scientific,
464 Bremen, DE) equipped with a robotic nanoflow ion source TriVersa NanoMate (Advion
465 BioSciences, Ithaca, USA) using nanoelectrospray chips with a diameter of 4.1 µm. The ion
466 source was controlled by the Chipsoft 8.3.1 software (Advion BioSciences). Ionization voltage
467 was + 0.96 kV in negative mode; backpressure was set at 1.25 psi. The temperature of the ion
468 transfer capillary was 200°C; S-lens RF level was set to 50%. FT MS spectra were acquired
469 within the range of m/z 50–750 at the mass resolution of R m/z 200 = 140000; automated gain
470 control (AGC) of 3×10^6 and with the maximal injection time of 3000 ms. FT MS/MS spectra
471 were acquired within the range of m/z 50–750 at the mass resolution of R m/z 200 = 140000;
472 automated gain control (AGC) of 3×10^4 and with the maximal injection time of 30 s.
473
474 **Triacylglycerols measurement from *Panagrolaimus n. sp* lysates**
475 Non-preconditioned and preconditioned pellets were lysed in 200 µl of isopropanol with 0.5
476 mm Zirconium beads twice for 15 min. The lysates were centrifuged at 1300 g for 5 min. The
477 supernatant was carefully collected without any debris, 20 µl of the lysate was used for protein
478 estimation. Normalization was performed according to soluble protein levels, supernatant

479 volumes corresponding to 50-100 µg of proteins were dried in the desiccator. 700 µl of IS
480 ((10:3 (Methyl tert-butyl ether: ethanol)) mix (warmed to room temperature) was added to
481 dried samples and left on a shaker for 1 hour. The samples were centrifuged at 1400 rpm and
482 4°C. 140 µl of water was added and left on shaker for 15 min. These samples were centrifuged
483 at 13400 rpm for 15 min. The upper organic fraction was collected and transferred to 1.5 ml
484 glass vial and left for drying in the desiccator. The dried samples were reconstituted in
485 appropriate volume of 300 µl of 4:2:1 (Isopropanol:Methanol:Chloroform) and volume
486 corresponding 1 µg was used for injection.
487 LC-MS/MS analysis was performed on a high-performance liquid chromatography
488 system (Agilent 1200 HPLC) coupled to a Xevo G2-S QTof (Waters). The samples were
489 resolved on a reverse phase C18 column (Cortecs C18 2.7um from Waters) with 50:50:0.1:1%
490 (Water:methanol:formic acid: 1M Ammonium formate) and 25:85:0.1:1%
491 (Acetonitrile:Isopropanol:Formic acid:1M Ammonium formate) as mobile phase. The
492 following gradient program was used: Eluent B from 0 % to 100 % within 12 min; 100 % from
493 12 min to 17min; 0 % from 17 min to 25 min. The flow rate was set at 0.3 ml/min. The samples
494 were normalised according to the total protein concentration and the worm numbers. TGD
495 50:00:00 was used as internal standard. Skyline software was used to analyse the raw data. The
496 TG were extracted from Lipidmaps database.
497
498
499
500
501
502
503
504
505
506
507
508
509
510
511
512

513 **Author contributions**

514 AS, VG, PS, TK conceived and designed the study. AS, VG, TH, MP, AT, GH, MH, ER, PS
515 and TK contributed to the original draft. AS performed isolation and cultivation of nematodes.
516 VG performed desiccation survival assays, trehalose measurement, 2D-TLC of metabolites,
517 trehalose-6-phosphate detection, combination of cryptobiosis experiments, genomic DNA
518 isolation from *Panagrolaimus n. sp*, assembled the data from all the authors and prepared the
519 figures. MP performed genome assembly. TH conducted orthology analyses and single gene
520 phylogenies and worked on figures. AT provided morphological description, light, and
521 scanning electron microscopy. LS analyzed the genome assembly and created figures. GMH
522 performed the phylogenetic analyses. ST performed triacylglycerols measurements, trehalose-
523 6-phosphate detection with suggestions from Andrej Shevchenko. MH annotated
524 supplementary table 3. PS performed genome annotation and supervised TH and LS. EWM
525 supervised MP and had overall responsibility for sequencing and assembly including funding
526 it.
527
528
529
530
531
532
533
534
535
536
537
538
539
540
541
542
543
544
545

Acknowledgements

VG is thankful to Andrej Shevchenko, members of Kurzchalia lab for helpful discussions and core facilities of MPI-CBG for assistance. We are grateful to Dr. S. Gubin for field study and sampling, our colleagues in Soil Cryology Lab, Pushchino and North-East Scientific Station in Chersky, Republic of Sakha (Yakutia) for their help and cooperation. The authors thank Long Read Team of the DRESDEN-concept Genome Center, DFG NGS Competence Center, part of the Center for Molecular and Cellular Bioengineering (CMCB), Technische Universität Dresden and MPI-CBG. GMH is funded by a UCD Ad Astra Fellowship. This work was supported by the Russian Foundation for Basic Research (19-29-05003-mk) to AS and ER. VG and TK acknowledge the financial support from the Volkswagen Foundation (Life? research grant 92847). PS and TH are supported by a DFG ENP grant to PS (DFG project 434028868). The authors are thankful to Richard Roy and Jens Bast for critical reading the manuscript. We thank Iain Pattern for suggestions in writing the manuscript. The funders have no role in the design of the study.

Conflict of interest:

The authors declare they have no conflict of interest relating to the content of this article.

References

1. Hibshman, J. D., Clegg, J. S. & Goldstein, B. Mechanisms of Desiccation Tolerance: Themes and Variations in Brine Shrimp, Roundworms, and Tardigrades. *Front. Physiol.* **11**, 592016 (2020).
2. Erkut, C. *et al.* Molecular Strategies of the Caenorhabditis elegans Dauer Larva to Survive Extreme Desiccation. *PLoS ONE* **8**, e82473 (2013).
3. Gade, V. R., Traikov, S., Oertel, J., Fahmy, K. & Kurzchalia, T. V. C. elegans possess a general program to enter cryptobiosis that allows dauer larvae to survive different kinds of abiotic stress. *Sci. Rep.* **10**, 13466 (2020).
4. Shatilovich, A. V. *et al.* Viable Nematodes from Late Pleistocene Permafrost of the Kolyma River Lowland. *Dokl. Biol. Sci.* **480**, 100–102 (2018).
5. Shmakova, L. *et al.* A living bdelloid rotifer from 24,000-year-old Arctic permafrost. *Curr. Biol.* **31**, R712–R713 (2021).
6. Keilin, D. The Leeuwenhoek Lecture - The problem of anabiosis or latent life: history and current concept. *Proc. R. Soc. Lond. Ser. B - Biol. Sci.* **150**, 149–191 (1959).
7. Cano, R. & Borucki, M. Revival and identification of bacterial spores in 25- to 40-million-year-old Dominican amber. *Science* **268**, 1060–1064 (1995).
8. Shen-Miller, J. Sacred lotus, the long-living fruits of China Antique. *Seed Sci. Res.* **12**, 131–143 (2002).
9. Guidetti, R. & Jönsson, K. I. Long-term anhydrobiotic survival in semi-terrestrial micrometazoans. *J. Zool.* **257**, 181–187 (2002).
10. Tsujimoto, M., Imura, S. & Kanda, H. Recovery and reproduction of an Antarctic tardigrade retrieved from a moss sample frozen for over 30 years. *Cryobiology* **72**, 78–81 (2016).
11. Kagoshima, H. *et al.* Multi-decadal survival of an Antarctic nematode, Plectus murrayi, in a -20°C stored moss sample. 9.
12. Aroian, R. V., Carta, L., Kaloshian, I. & Sternberg, P. W. A Free - living Panagrolaimus sp. from Armenia Can Survive in Anhydrobiosis for 8.7 Years. 3.
13. Gilichinsky, D. A. *et al.* Microbial Populations in Antarctic Permafrost: Biodiversity, State, Age, and Implication for Astrobiology. *Astrobiology* **7**, 275–311 (2007).
14. Rivkina, E. *et al.* Earth's perennially frozen environments as a model of cryogenic planet ecosystems. *Permafr. Periglac. Process.* **29**, 246–256 (2018).
15. Sipes, K. *et al.* Eight Metagenome-Assembled Genomes Provide Evidence for Microbial Adaptation in 20,000- to 1,000,000-Year-Old Siberian Permafrost. *Appl. Environ. Microbiol.* **87**, (2021).

657 16.Liang, R. *et al.* Genomic reconstruction of fossil and living microorganisms in ancient
658 Siberian permafrost. *Microbiome* **9**, 110 (2021).
659 17.Gilichinsky, D. A. & Rivkina, E. M. Permafrost microbiology. 7 (2011).
660 18.Yashina, S. *et al.* Regeneration of whole fertile plants from 30,000-y-old fruit tissue buried
661 in Siberian permafrost. *Proc. Natl. Acad. Sci.* **109**, 4008–4013 (2012).
662 19.Adhikari, B. N., Wall, D. H. & Adams, B. J. Desiccation survival in an Antarctic nematode:
663 molecular analysis using expressed sequenced tags. *BMC Genomics* **10**, 69 (2009).
664 20.Tyson, T. *et al.* A molecular analysis of desiccation tolerance mechanisms in the
665 anhydrobiotic nematode Panagrolaimus superbus using expressed sequenced tags. *BMC Res.*
666 *Notes* **5**, 68 (2012).
667 21.McGill, L. M. *et al.* Anhydrobiosis and Freezing-Tolerance: Adaptations That Facilitate the
668 Establishment of Panagrolaimus Nematodes in Polar Habitats. *PLOS ONE* **10**, e0116084
669 (2015).
670 22.Thorne, M. A. S., Kagoshima, H., Clark, M. S., Marshall, C. J. & Wharton, D. A. Molecular
671 Analysis of the Cold Tolerant Antarctic Nematode, Panagrolaimus davidi. *PLoS ONE* **9**,
672 e104526 (2014).
673 23.Sandhove, J., Spann, N. & Ristau, K. The Anhydrobiotic Potential of the Terrestrial
674 Nematodes *Plectus parietinus* and *Plectus velox*: Anhydrobiosis of *plectus parietinus* and *p.*
675 *velox*. *J. Exp. Zool. Part Ecol. Genet. Physiol.* **325**, 434–440 (2016).
676 24.Erkut, C. *et al.* Trehalose Renders the Dauer Larva of Caenorhabditis elegans Resistant to
677 Extreme Desiccation. *Curr. Biol.* **21**, 1331–1336 (2011).
678 25.Erkut, C., Gade, V. R., Laxman, S. & Kurzchalia, T. V. The glyoxylate shunt is essential
679 for desiccation tolerance in C. elegans and budding yeast. *elife* **5**, (2016).
680 26.Zanina, O. G., Gubin, S. V., Kuzmina, S. A., Maximovich, S. V. & Lopatina, D. A. Late-
681 Pleistocene (MIS 3-2) palaeoenvironments as recorded by sediments, palaeosols, and
682 ground-squirrel nests at Duvanny Yar, Kolyma lowland, northeast Siberia. *Quat. Sci. Rev.*
683 **30**, 2107–2123 (2011).
684 27.Murton, J. B. *et al.* Palaeoenvironmental Interpretation of Yedoma Silt (Ice Complex)
685 Deposition as Cold-Climate Loess, Duvanny Yar, Northeast Siberia: Palaeoenvironmental
686 Interpretation of Yedoma Silt, Duvanny Yar. *Permafr. Periglac. Process.* **26**, 208–288
687 (2015).
688 28.Abramov, A., Vishnivetskaya, T. & Rivkina, E. Are permafrost microorganisms as old as
689 permafrost? *FEMS Microbiol. Ecol.* **97**, fiaa260 (2021).

690 29.Gilichinsky, D. A., Wagener, S. & Vishnevetskaya, T. A. Permafrost microbiology.
691 *Permafr. Periglac. Process.* **6**, 281–291 (1995).
692 30.Schiffer, P. H. *et al.* Signatures of the Evolution of Parthenogenesis and Cryptobiosis in the
693 Genomes of Panagrolaimid Nematodes. *iScience* **21**, 587–602 (2019).
694 31.Schiffer, P. H. *et al.* Developmental variations among Panagrolaimid nematodes indicate
695 developmental system drift within a small taxonomic unit. *Dev. Genes Evol.* **224**, 183–188
696 (2014).
697 32.Dey, A., Chan, C. K. W., Thomas, C. G. & Cutter, A. D. Molecular hyperdiversity defines
698 populations of the nematode Caenorhabditis brenneri. *Proc. Natl. Acad. Sci.* **110**, 11056–
699 11060 (2013).
700 33.Cutter, A. D. Divergence Times in Caenorhabditis and Drosophila Inferred from Direct
701 Estimates of the Neutral Mutation Rate. *Mol. Biol. Evol.* **25**, 778–786 (2008).
702 34.Malavin, S., Shmakova, L., Claverie, J.-M. & Rivkina, E. Frozen Zoo: a collection of
703 permafrost samples containing viable protists and their viruses. *Biodivers. Data J.* **8**, e51586
704 (2020).
705 35.Krivushin, K. *et al.* Two Metagenomes from Late Pleistocene Northeast Siberian
706 Permafrost. *Genome Announc.* **3**, e01380-14 (2015).
707 36.Zhou, J. *et al.* Phylogenetic diversity of a bacterial community determined from Siberian
708 tundra soil DNA. *Microbiology* **143**, 3913–3919 (1997).
709 37.Kapterev, P. Anabiosis in the conditions of permanent congelation. *Izv Akad Nauk SSSR Ser*
710 *Biol* **6**, 1073–1088 (1936).
711 38.Kapterev, P. New data on revitalization of organisms from perpetually frozen grounds. *CR*
712 *Acad Sci URSS* **20**, 315–317 (1938).
713 39.Andrássy, I. *Klasse Nematoda*. (Gustav Fischer Verlag, 1984).
714 40.Lewis, S. C. *et al.* Molecular evolution in Panagrolaimus nematodes: origins of
715 parthenogenesis, hermaphroditism and the Antarctic species P. davidi. *BMC Evol. Biol.* **9**,
716 15 (2009).
717 41.Andrássy, I. *Free-living Nematodes of Hungary*. (Hungarian Natural History Museum,
718 2005).
719 42.Schulenburg, H. & Félix, M.-A. The Natural Biotic Environment of *Caenorhabditis elegans*.
720 *Genetics* **206**, 55–86 (2017).
721 43.Frézal, L. & Félix, M.-A. C. elegans outside the Petri dish. *eLife* **4**, e05849 (2015).
722 44.Gems, D. *et al.* Two pleiotropic classes of daf-2 mutation affect larval arrest, adult behavior,
723 reproduction and longevity in Caenorhabditis elegans. *Genetics* **150**, 129–155 (1998).

724 45.Vowels, J. J. & Thomas, J. H. Multiple chemosensory defects in daf-11 and daf-21 mutants
725 of Caenorhabditis elegans. *Genetics* **138**, 303–316 (1994).
726 46.Ren Peifeng *et al.* Control of C. elegans Larval Development by Neuronal Expression of a
727 TGF-β Homolog. *Science* **274**, 1389–1391 (1996).
728 47.Gerisch, B., Weitzel, C., Kober-Eisermann, C., Rottiers, V. & Antebi, A. A Hormonal
729 Signaling Pathway Influencing C. elegans Metabolism, Reproductive Development, and
730 Life Span. *Dev. Cell* **1**, 841–851 (2001).
731 48.Penkov, S. *et al.* Integration of carbohydrate metabolism and redox state controls dauer
732 larva formation in Caenorhabditis elegans. *Nat. Commun.* **6**, 8060 (2015).
733 49.Penkov, S. *et al.* A metabolic switch regulates the transition between growth and diapause
734 in C. elegans. *BMC Biol.* **18**, 31 (2020).
735 50.Nurk, S. *et al.* HiCanu: accurate assembly of segmental duplications, satellites, and allelic
736 variants from high-fidelity long reads. *Genome Res.* **30**, 1291–1305 (2020).
737 51.Brůna, T., Hoff, K. J., Lomsadze, A., Stanke, M. & Borodovsky, M. BRAKER2: automatic
738 eukaryotic genome annotation with GeneMark-EP+ and AUGUSTUS supported by a
739 protein database. *NAR Genomics Bioinforma.* **3**, lqaa108 (2021).
740 52.Smythe, A. B., Holovachov, O. & Kocot, K. M. Improved phylogenomic sampling of free-
741 living nematodes enhances resolution of higher-level nematode phylogeny. *BMC Evol. Biol.*
742 **19**, 121 (2019).
743 53.Ahmed, M., Adedidran, F. & Holovachov, O. A draft transcriptome of a parasite
744 Neocamacolaimus parasiticus (Camacolaimidae, Plectida). *J. Nematol.* **53**, 1–4 (2021).
745 54.Grabherr, M. G. *et al.* Full-length transcriptome assembly from RNA-Seq data without a
746 reference genome. *Nat. Biotechnol.* **29**, 644–652 (2011).
747 55.Goecks, J., Nekrutenko, A., Taylor, J. & Galaxy Team, T. Galaxy: a comprehensive
748 approach for supporting accessible, reproducible, and transparent computational research in
749 the life sciences. *Genome Biol.* **11**, R86 (2010).
750 56.Haas, B. J. *et al.* De novo transcript sequence reconstruction from RNA-seq using the
751 Trinity platform for reference generation and analysis. *Nat. Protoc.* **8**, 1494–1512 (2013).
752 57.Li, W. & Godzik, A. Cd-hit: a fast program for clustering and comparing large sets of
753 protein or nucleotide sequences. *Bioinformatics* **22**, 1658–1659 (2006).
754 58.Fu, L., Niu, B., Zhu, Z., Wu, S. & Li, W. CD-HIT: accelerated for clustering the next-
755 generation sequencing data. *Bioinformatics* **28**, 3150–3152 (2012).

59. Emms, D. M. & Kelly, S. OrthoFinder: solving fundamental biases in whole genome comparisons dramatically improves orthogroup inference accuracy. *Genome Biol.* **16**, 157 (2015).
60. Emms, D. M. & Kelly, S. OrthoFinder: phylogenetic orthology inference for comparative genomics. *Genome Biol.* **20**, 238 (2019).
61. Katoh, K. & Standley, D. M. MAFFT Multiple Sequence Alignment Software Version 7: Improvements in Performance and Usability. *Mol. Biol. Evol.* **30**, 772–780 (2013).
62. Capella-Gutierrez, S., Silla-Martinez, J. M. & Gabaldon, T. trimAl: a tool for automated alignment trimming in large-scale phylogenetic analyses. *Bioinformatics* **25**, 1972–1973 (2009).
63. Minh, B. Q. *et al.* IQ-TREE 2: New Models and Efficient Methods for Phylogenetic Inference in the Genomic Era. *Mol. Biol. Evol.* **37**, 1530–1534 (2020).
64. Jones, P. *et al.* InterProScan 5: genome-scale protein function classification. *Bioinformatics* **30**, 1236–1240 (2014).
65. Huson, D. H. & Scornavacca, C. Dendroscope 3: An Interactive Tool for Rooted Phylogenetic Trees and Networks. *Syst. Biol.* **61**, 1061–1067 (2012).
66. Kück, P. & Meusemann, K. FASconCAT: Convenient handling of data matrices. *Mol. Phylogenet. Evol.* **56**, 1115–1118 (2010).
67. Nguyen, L.-T., Schmidt, H. A., von Haeseler, A. & Minh, B. Q. IQ-TREE: A Fast and Effective Stochastic Algorithm for Estimating Maximum-Likelihood Phylogenies. *Mol. Biol. Evol.* **32**, 268–274 (2015).
68. Kalyaanamoorthy, S., Minh, B. Q., Wong, T. K. F., von Haeseler, A. & Jermiin, L. S. ModelFinder: fast model selection for accurate phylogenetic estimates. *Nat. Methods* **14**, 587–589 (2017).
69. Zhang, C., Scornavacca, C., Molloy, E. K. & Mirarab, S. ASTRAL-Pro: Quartet-Based Species-Tree Inference despite Paralogy. *Mol. Biol. Evol.* **37**, 3292–3307 (2020).
70. Ranallo-Benavidez, T. R., Jaron, K. S. & Schatz, M. C. GenomeScope 2.0 and Smudgeplot for reference-free profiling of polyploid genomes. *Nat. Commun.* **11**, 1432 (2020).
71. Kokot, M., Długosz, M. & Deorowicz, S. KMC 3: counting and manipulating k-mer statistics. *Bioinformatics* **33**, 2759–2761 (2017).

Figure legends

Figure 1. Study site.

a) location of the Duvanny Yar outcrope on the Kolyma River, northeastern Siberia, Russia. b) view of the upper part of outcrop composed of ice wedges and permafrost silty deposits. c) lithostratigraphic scheme of deposits, showing location of studied rodent borrow (red circle). d) fossil rodent burrow with herbaceous litter and seeds buried in permafrost deposits; m a.r.l. = meters above river level.

Figure 2. General morphology of *Panagrolaimus n. sp* sp. n., female.

Scanning electron pictures (a, c), light microscopy photographs (e, f) and graphic presentations (b, d, g) of holotype: a, b) entire body, c, d) anterior ends, e) anterior body, f) perivulvar body region, g) tail. Abbreviations: l.f. – lateral field, ov – ovary, pro – procorpus of the pharynx, t.b. – terminal bulb of the pharynx, u – uterus with eggs, v – vulva, v.p. – ventral pore. Scale bars: a, d, e, f, g – 20 µm, b – 100 µm, c – 2 µm.

Figure 3. Genome assembly and phylogenomics reveals that the newly discovered *Panagrolaimus n. sp* species is triploid.

a) Kmer spectra of the *Panagrolaimus n. sp* PacBio HiFi data. Kmers of length 19 were counted using Jellyfish. b) Circos plot showing the triploid structure of the *Panagrolaimus kolymensis* genome. The relationship between eight contigs, representing 39.9 Mb (15%) of the genome, is shown. Numbers represent the contig IDs. c) Inferred species tree for all taxa. The maximum likelihood tree inferred using a concatenated supermatrix (18S and 28S genes) with bootstrap support values is displayed. All genera are represented as monophyletic clades. *Panagrolaimus n. sp* is highlighted in red and basal to all other *Panagrolaimus* taxa. Internal nodes, where all subsequent branches represent identical sequences, are displayed with a black star. d) *Panagrolaimus n. sp.* possesses *C. elegans* gene orthologs to enzymes required for TCA cycle, glyoxylate shunt, glycolysis, gluconeogenesis, trehalose synthesis, and polyamine synthesis. Black filled circles: Ortholog presence suggested by orthogroup clustering, phylogenetic analysis, and domain architecture. White filled circles: No ortholog found via current analysis. Coloured filled circles: Presence of *Panagrolaimus n. sp.* gene(s), related to several *C. elegans* genes (all genes of same colour) that are all co-orthologous to that gene (those genes). Label: *C. elegans* enzyme names and orthogroup that contains that gene according to our orthogroup clustering.

888 **Figure 4. *C. elegans* dauer larvae and *Panagrolaimus n. sp.* utilize similar mechanisms to**
889 **survive cryptobiosis.**
890 a) Survival rate of *Panagrolaimus n. sp.* nematodes to desiccation and freezing (-80°C). Error
891 bars indicate standard error of mean of two independent experiments with two technical
892 replicates performed on two different days. Statistical comparison was performed using
893 unpaired t test with Welch correction. n.s. $p > 0.05$, ****$p < 0.0001$. For desiccation (non-
894 preconditioned) n = 289, freezing (non-preconditioned) n = 675, desiccation (preconditioned
895 at 98%RH) n = 953 and freezing (preconditioned at 98%RH) n = 1295. b) *Panagrolaimus n.*
896 *sp.* nematodes and *daf-2(e1370)* dauer larvae upregulate trehalose levels upon preconditioning
897 at 98%RH. Error bars indicate standard error of mean of two independent experiments with
898 three replicates performed on two different days. Statistical comparison was performed using
899 two-way ANOVA with Holm-Sidak's multiple comparison test, ****$p < 0.0001$. c-d) 2D-thin
900 layer chromatography of ^{14}C-acetate labelled metabolites from *Panagrolaimus n. sp.* that were
901 non-preconditioned and preconditioned at 98%RH. Enumerated spots indicate trehalose (1),
902 glucose (2), glutamate (3), glutamine (4), serine/glycine (5) and phenylalanine (6).
903 Representative images from at least two independent experiments performed on two different
904 days. e) Desiccated *daf-2 (e1370)* dauer larvae survive to freezing (-80°C) for an extremely
905 long period. Error bars indicate standard error of mean of two independent experiments with
906 two technical replicates performed on two different days. f) Brood size of desiccated dauer
907 larvae exposed to freezing remain like that non- desiccated dauer larvae. Average brood size is
908 the mean of seven dauer larvae per each condition. Statistical comparison was performed by
909 using non-parametric Kolmogorov-smirnov test n.s $p>0.05$.
910
911
912
913
914
915
916
917
918
919
920
921

Figure S1. Calibration of a radiocarbon (^{14}C) date.

Radiocarbon date (44,315±405 BP) and calibrated age (45,839 -- 47,769 cal BP) of plant material collected from buried borrow P-1320. Radiocarbon ages were converted to calendar age equivalents with the OxCal V.4.4 program using the IntCal20 calibration curve. Pink-shaded area — radiocarbon date with standard deviation; grey-shaded area — radiocarbon date projection on the calibration curve with 95.4% probability.

Figure S2. Morphology of *Panagrolaimus n. sp* sp. n., female.

Graphic presentations of holotype (a,b) and SEM pictures (c-i): a) anterior body, b) female reproductive branch, c–e) anterior end of three different female specimens, f) anterior part of the lateral ridge, g) vulva, h) ventral excretory/secretory pore, i) posterior body with anus and lateral ridge. Scale bars: a,b - 50 µm, c,i - 3 µm, d - 2 µm, e –1 µm, f,h - 5 µm, g - 10 µm, .

Figure S3. Phylogenies inferred for genes sets using both concatenation and coalescence approaches.

a) The ploidy level was analysed with *Smudgeplot* v0.2.1[70]. KMC version 3.1.0[71] was used to count the 21-mers in the PacBio CCS reads. Then we ran *smudgeplot.py* to determine the lower and upper coverage cut-offs. These were determined to be 14 and 380. 21-mers with a coverage between 14 and 380 were filtered with kmc_tools. Then, we computed the k-mer pairs from the filtered 21-mers by running *smudgeplot.py hetkmers*. Finally, the produced a smudgeplot shows an estimated ploidy of 3. b) Species tree inferred for 12,295 gene trees using a coalescence approach. The species tree implemented using the coalescence approach with orthogroup gene trees is displayed. Novel species in this study are displayed in red. All nodes have a posterior probability of 1. c) Species tree inferred for 102 taxa**.** The maximum likelihood tree inferred using a concatenated supermatrix of 60 genes is displayed. Bootstrap values are only displayed for nodes with less than 100% support. The platyhelminth *Macrostum lignano* serves as an outgroup for rooting. The ancestral *Panagrolaimus*, sister to all others within the *Panagrolaimus* genus, is highlighted in red.

1021 **Figure S4. Combination of cryptobiotic states enhances survival of *C. elegans* dauer**
1022 **larvae.**
1023 a) Desiccated dauer larvae manifest enhanced survival rate to heat stress (34°C). Error bars
1024 indicate standard deviation of two independent experiments with two technical replicates. b)
1025 Desiccated dauer larvae display enhances survival rate to anoxia. Error bars indicate standard
1026 deviation of two independent experiments with two technical replicates. Statistical
1027 comparison was performed by paired two tailed t-test. *$p<0.05$. c) *Panagrolaimus n. sp.*
1028 possesses gene orthologs to most genes implicated in dauer formation and metabolism in *C.*
1029 *elegans*. Black filled circles: Ortholog presence suggested by orthogroup clustering,
1030 phylogenetic analysis, and domain architecture. White filled circles: No ortholog found via
1031 current analysis (in all cases these *C. elegans* genes did not cluster with any *Panagrolaimus*
1032 genes in the orthogroup clustering). Label: *C. elegans* enzyme names and orthogroup that
1033 contains that gene according to our orthogroup clustering.
1034
1035
1036
1037
1038
1039
1040
1041
1042
1043
1044
1045
1046
1047
1048
1049
1050
1051
1052
1053
1054

1055 **Figure S5. *Panagrolaimus n. sp.* reduces triacylglycerols (TAGs) levels and accumulates**
1056 **trehalose-6-phosphate upon preconditioning at 98%RH**.
1057 a) 1D-Thin layer chromatography of acetate labelled organic fractions of non-preconditioned
1058 (1) and preconditioned (2) *P. kolymaensis*. b) Mass spectrometric quantification of TAG levels
1059 of non-preconditioned (1) and preconditioned (2) *P. kolymaensis*. Error bars indicate standard
1060 deviation of two independent experiments with two technical replicates. Statistical analysis
1061 was performed using unpaired t-test with Welch correction **$p < 0.001$. c-d) non-
1062 preconditioned and preconditioned mass spectrum of an empty region, e-f) spot 1 (trehalose),
1063 g-f) spot 7 (trehalose-6-phosphate) scraped out and extracted from the 2D-TLC.
1064
1065
1066
1067
1068
1069
1070
1071
1072
1073
1074
1075
1076
1077
1078
1079
1080
1081
1082
1083
1084

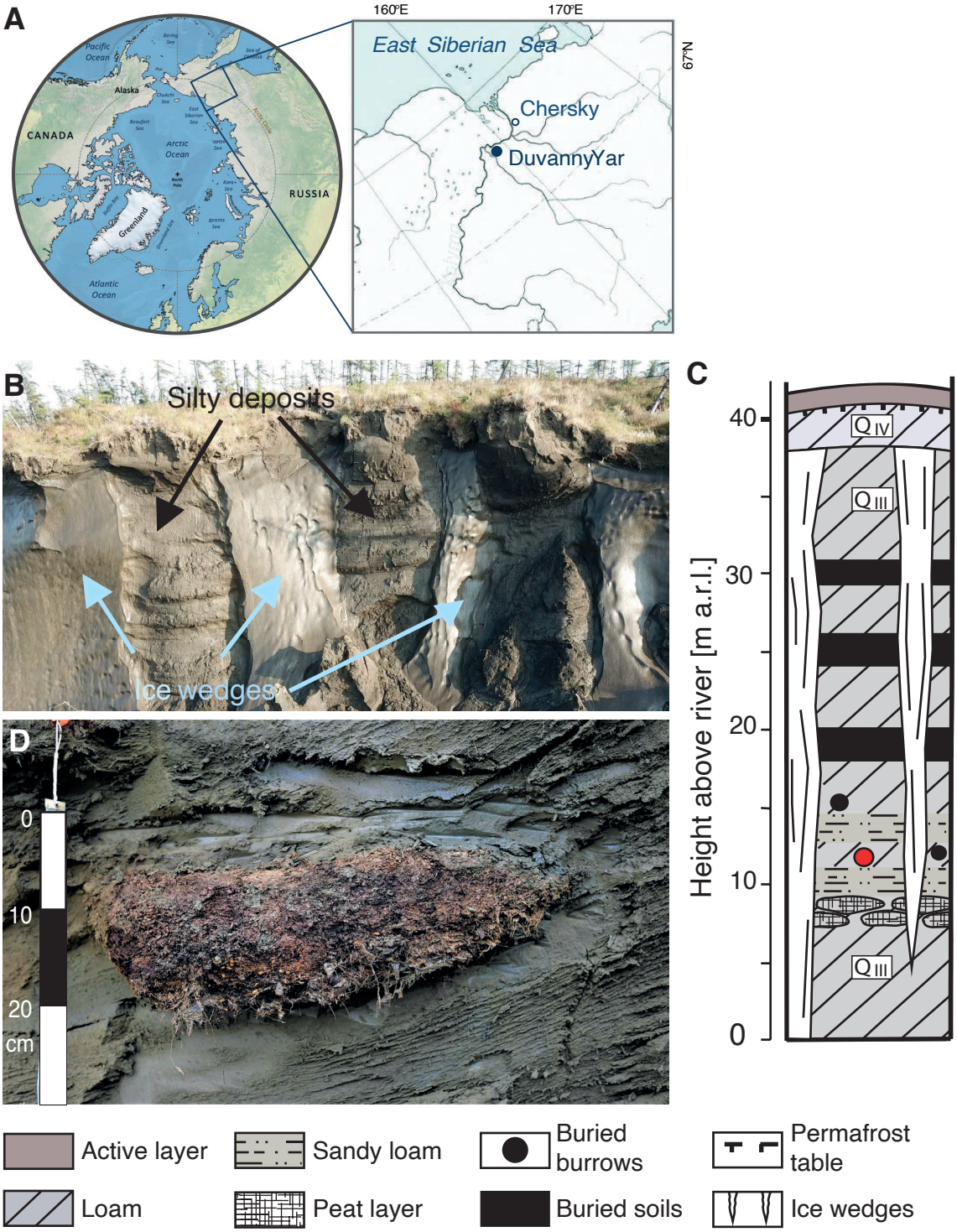

Figure 1
Shatilovich *et al*

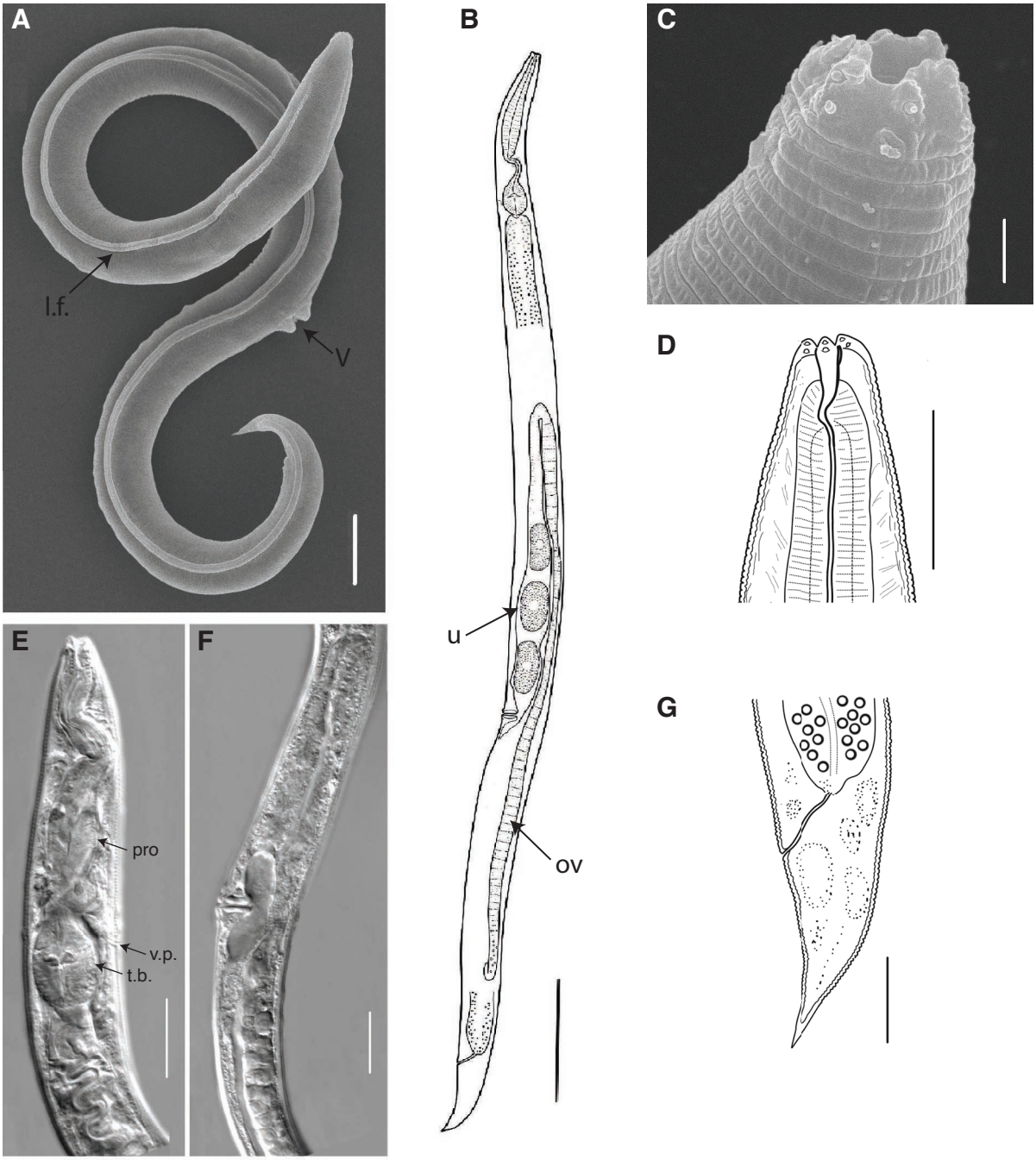

Figure 2
Shatilovich *et al*

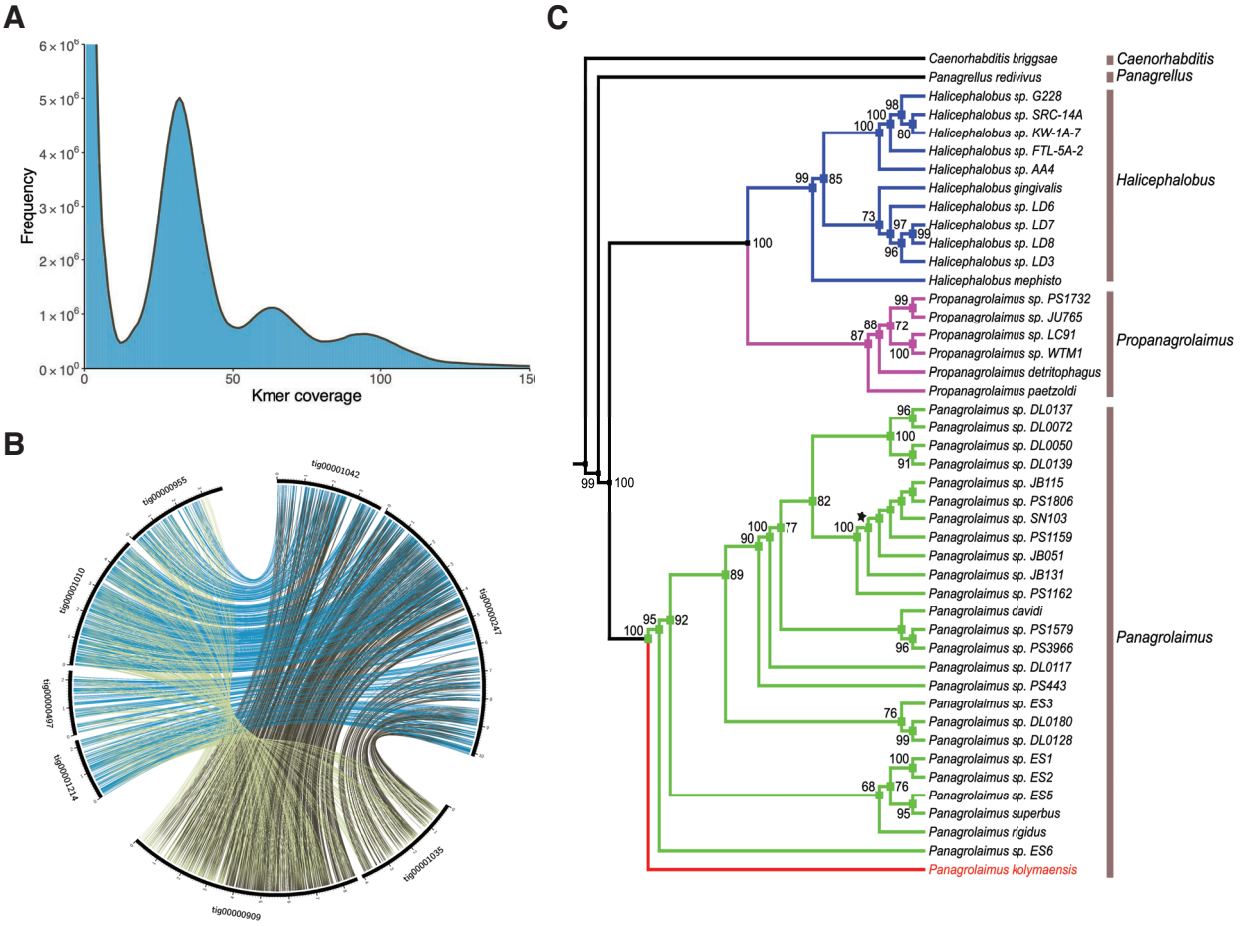

Figure 3
Shatilovich *et al*

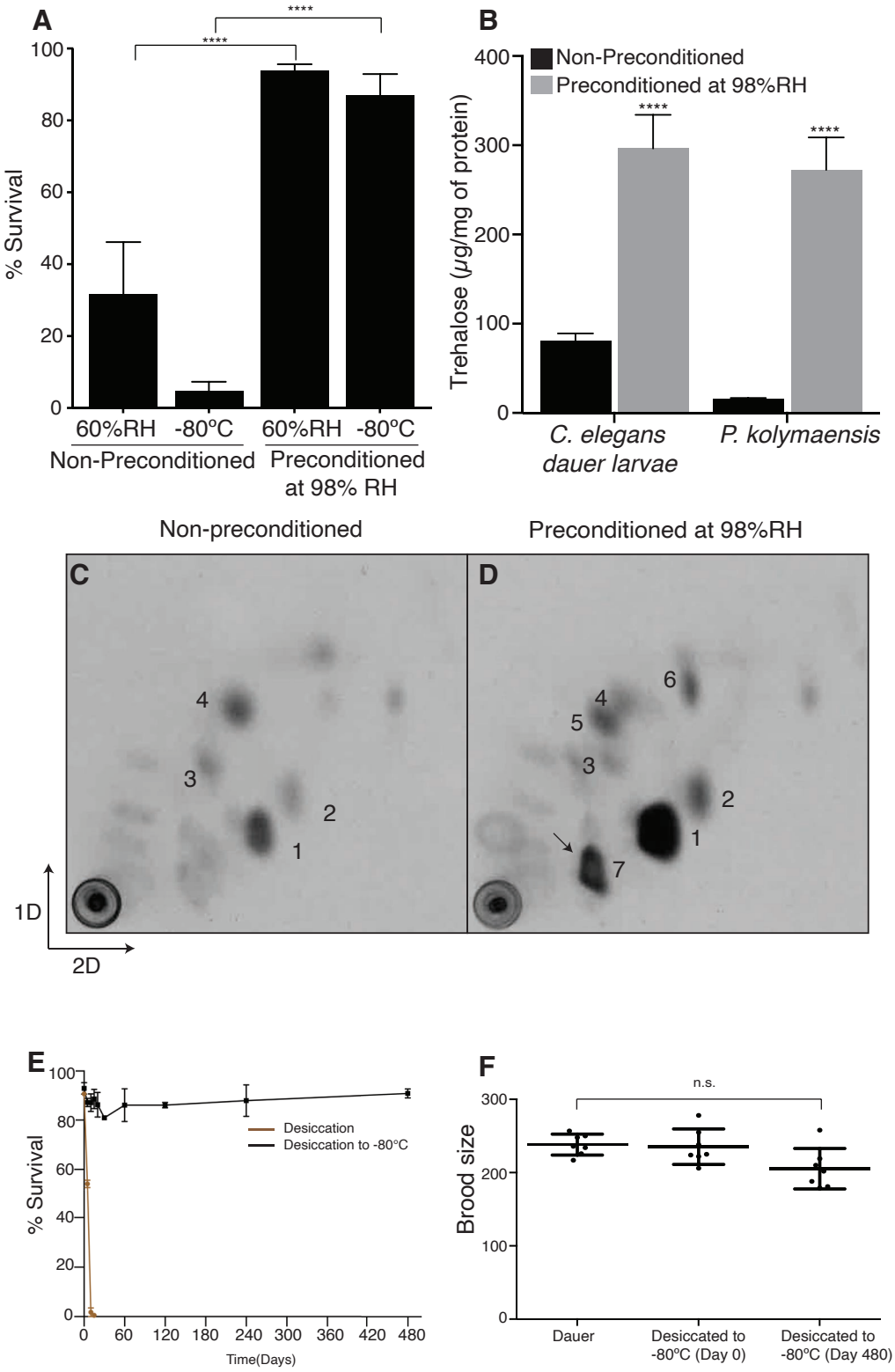

Figure 4
Shatilovich *et al*

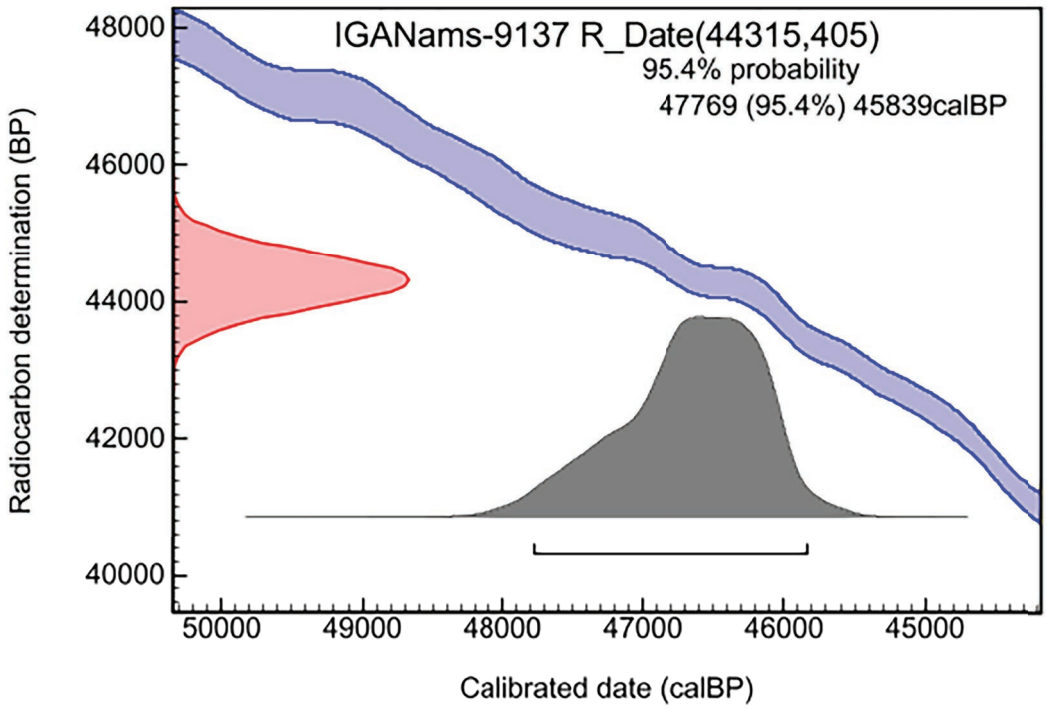

Figure S1
Shatilovich *et al*

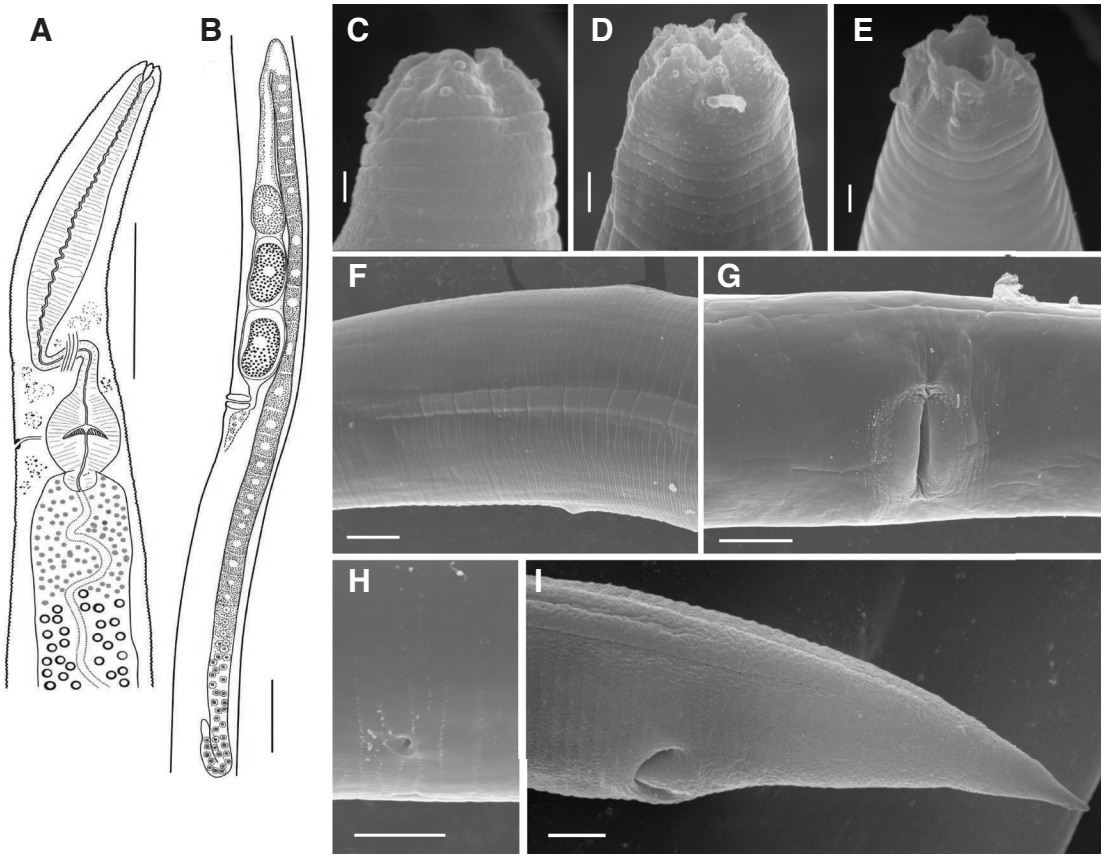

Figure S2
Shatilovich *et al*

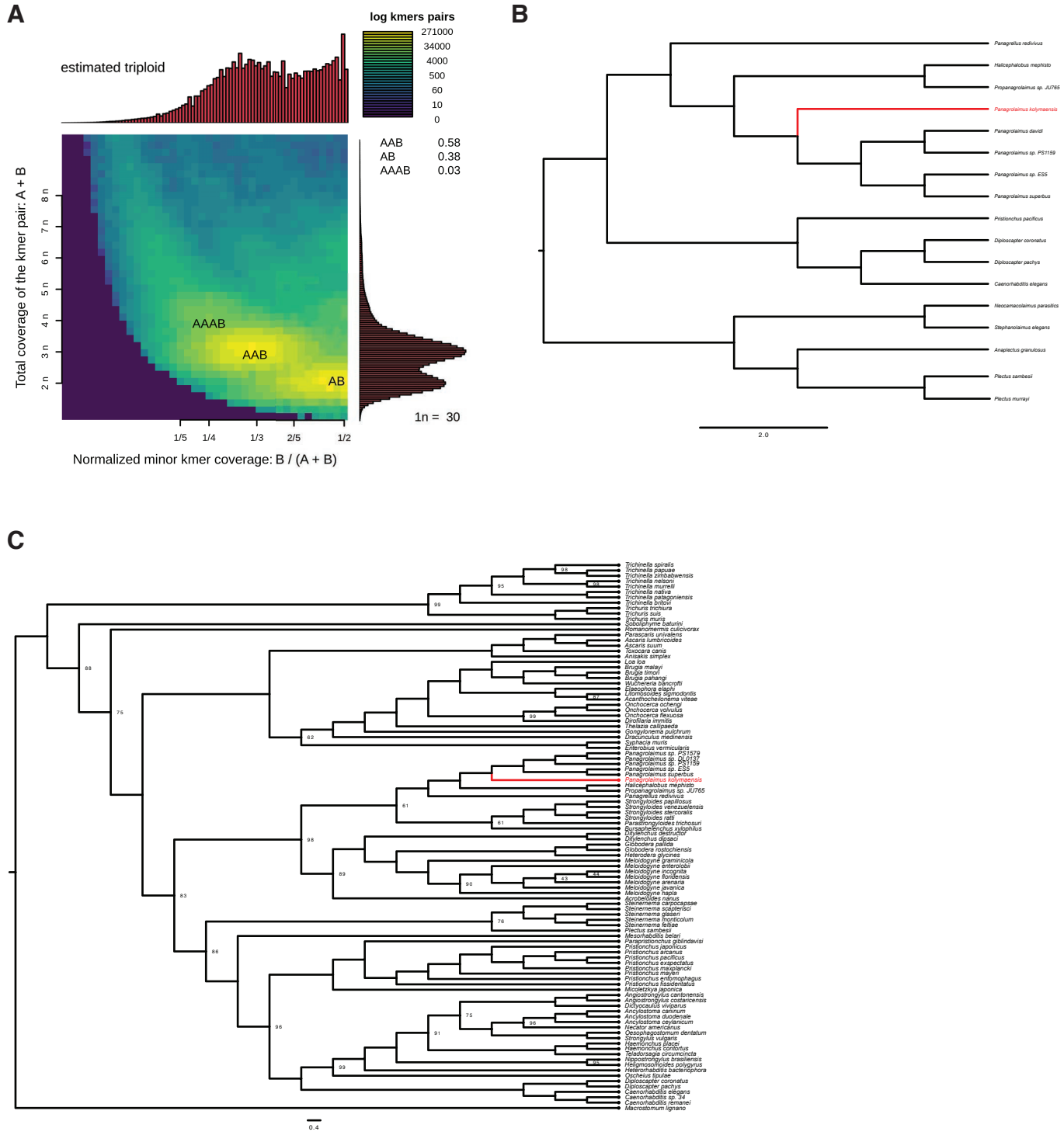

Figure S3
Shatilovich *et al*

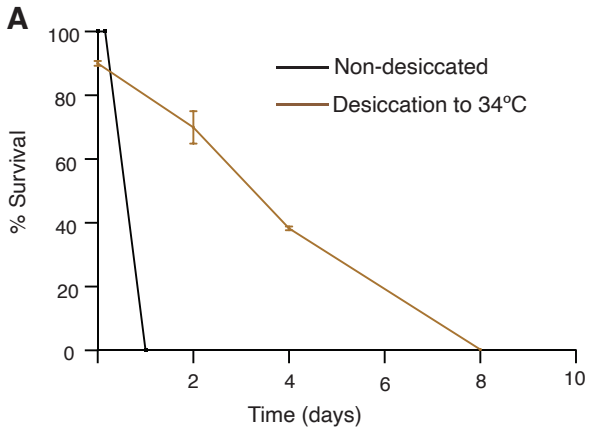

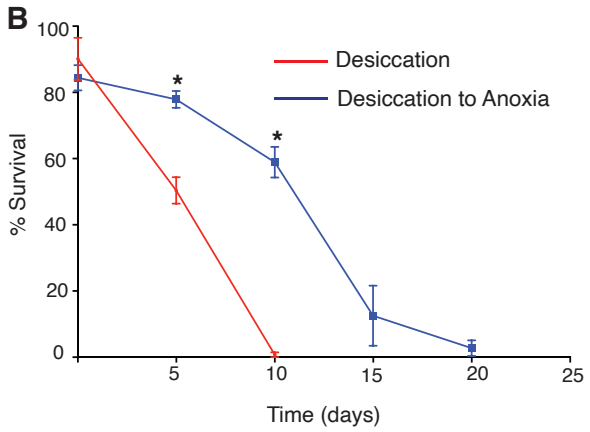

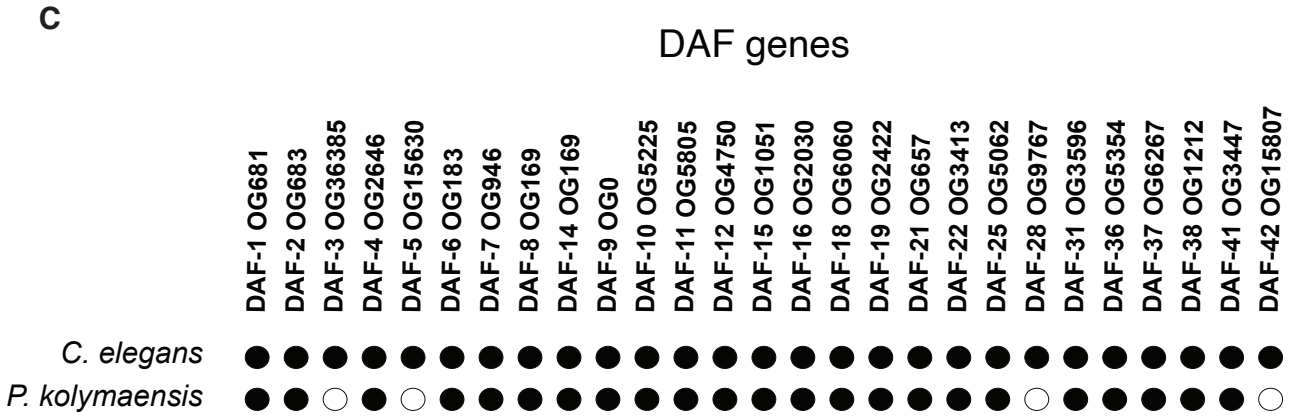

Figure S4
Shatilovich *et al*

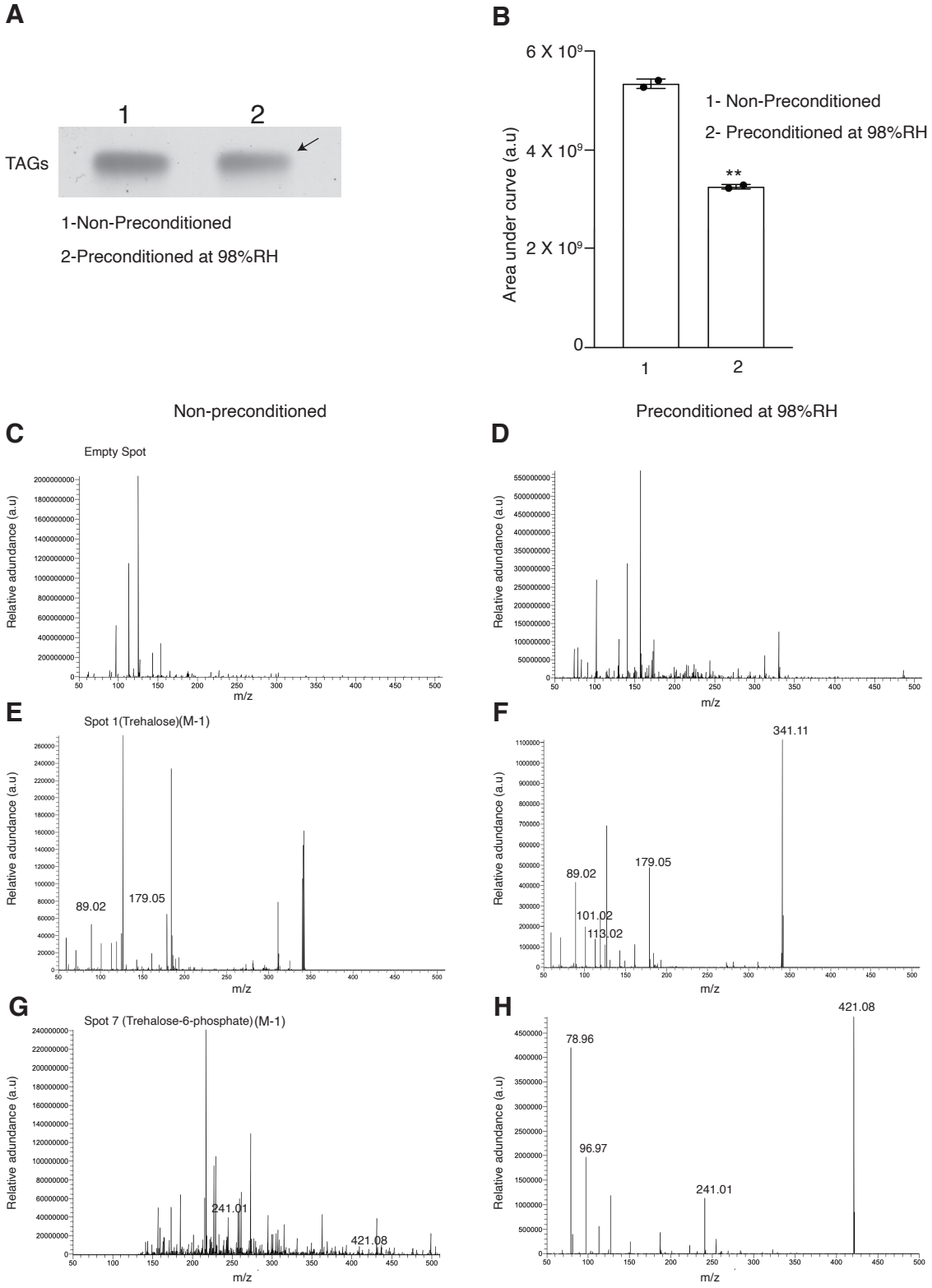

Figure S5
Shatilovich *et al*